

CRS09A Technical Datasheet

Analogue Angular Rate Sensor

High Performance MEMS Gyroscope

SILICON SENSING 

www.siliconsensing.com



Features

- Proven and Robust silicon MEMS vibrating ring structure
- FOG-like performance
- Low Bias Instability
- Excellent Angle Random Walk
- Low noise
- Precision analogue output
- Wide range from -40°C to +85°C
- High shock and vibration rejection
- Temperature sensor output for precision thermal compensation
- MEMS frequency output for precision thermal compensation
- RoHS Compliant
- Two rate ranges, two performance options for each

Applications

- Platform Stabilisation
- Precision Surveying
- Maritime Guidance and Control
- Gyro-compassing and Heading Control
- Autonomous Vehicles and ROVs
- Rail Track monitoring
- Robotics

1 General Description

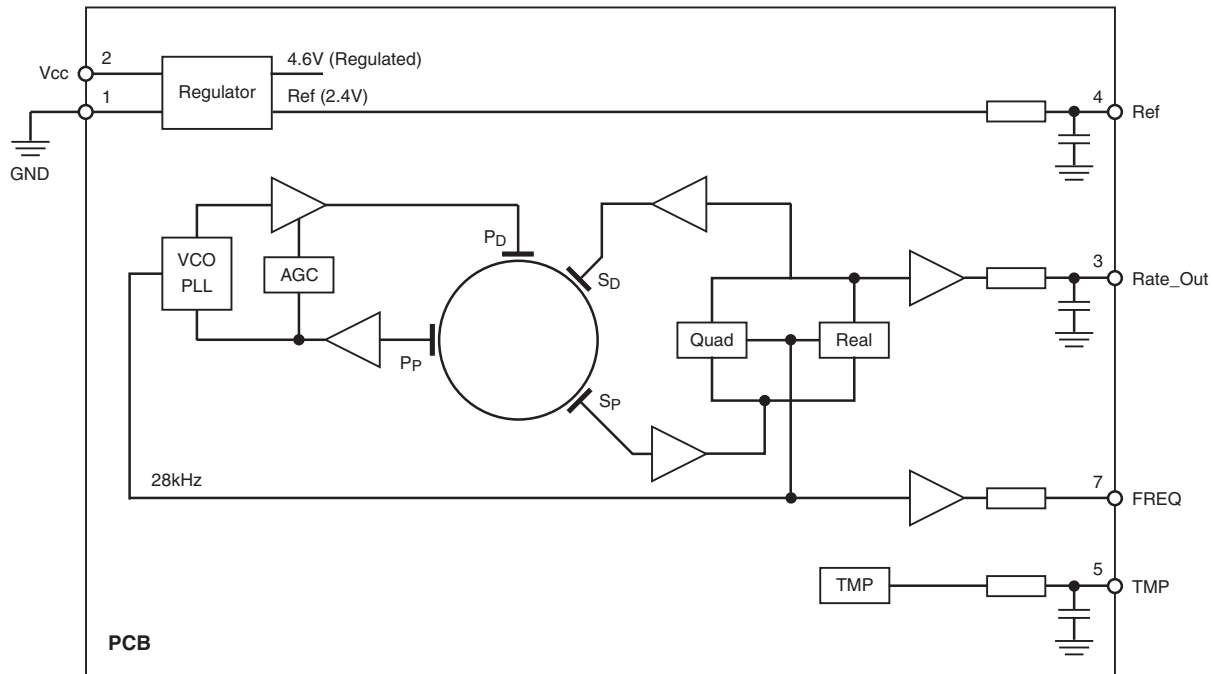
CRS09A provides the optimum solution for rate range applications where bias instability, angle random walk and low noise are of critical importance.

The latest inductive MEMS gyro sensor element is combined with precision discrete electronics to achieve high stability and low noise, making the CRS09A a viable alternative to fibre-optic and dynamically tuned gyros.

An on board temperature sensor and the resonant frequency of the MEMS enable additional external conditioning to be applied to the CRS09A by the host, enhancing the performance even further. Test data for Bias and Scale Factor can be provided with each gyroscope enabling this compensation to be implemented without the need for further calibration.

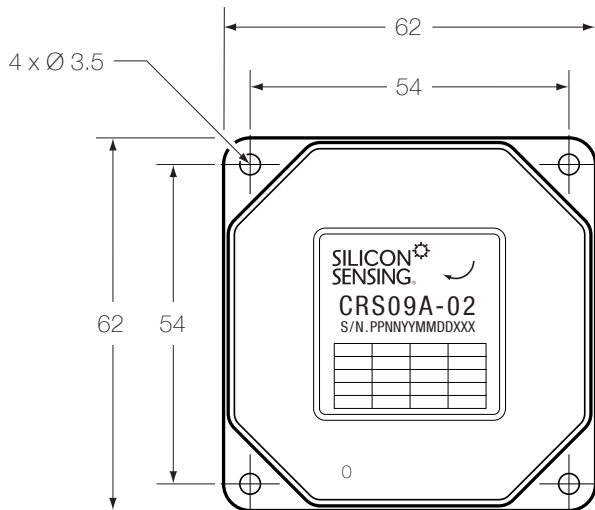
Typical applications include downhole surveying, precision platform stabilisation, ship stabilisation, ship guidance and control, autonomous vehicles and high-end AHRS.

Whatever your application, the unique and patented silicon ring technology gives advanced and stable performance over time and temperature, overcoming mount sensitivity problems associated with simple beam or tuning fork based sensors.



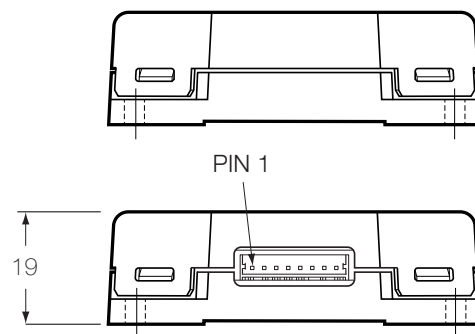
C.G.18633

Figure 1.1 CRS09A Functional Block Diagram



All dimensions in millimetres.

Mass: 60g



Connector: 53254-0870 (Molex)

Mating Connector: 51065-0800 (Molex). This connector with 500mm cable, is included with each CRS09A. See Figure 7.1b for correct wiring schedule.

NOTE: The identification of Pin 1 on the Molex connectors should be ignored. The CRS09A pinout as defined on the product label and the Pin 1 indent on the product lid must take precedent. See Figure 7.1a.

Figure 1.2 CRS09A Overall Dimensions

2 Ordering Information

Part Number	Rate Range	Bias Over Temperature	Notes
CRS09A-01	±200°/s	< ±3°/s	–
CRS09A-02	±100°/s	< ±3°/s	–
CRS09A-11	±200°/s	< ±1°/s	Optimal performance over temperature
CRS09A-12	±100°/s	< ±1°/s	Optimal performance over temperature
CRS09A-22	±100°/s	< ±1°/s	Reduced temperature range version

3 Specification

Unless otherwise specified the following specification values assume V_{dd} = 4.75 to 5.25V over the temperature range -40 to +85°C.

Parameter	CRS09A-01, CRS09A-11	CRS09A-02, CRS09A-12, CRS09A-22	Notes
Rate Range	±200°/s	±100°/s	–
Nominal Scale Factor	10mV/°/s	20mV/°/s	–
Scale Factor Setting Error	≤ ±1%	≤ ±1%	At nominal 23°C
Scale Factor Variation Over Temperature	≤ ±1%	≤ ±1%	Over specified operating temperature range
Non-Linearity	< 0.1%	< 0.1%	Of full scale range
Bias Setting Error	< ±10mV	< ±20mV	At nominal 23°C
Bias Variation Over Temperature Range	< ±3°/s (CRS09A-01) < ±1°/s (CRS09A-11)	< ±3°/s (CRS09A-02) < ±1°/s (CRS09A-12) < ±1°/s (CRS09A-22)	–
Angular Random Walk	< 0.1°/√hr	< 0.1°/√hr	At constant temperature using the Allan Variance method
Bias Instability	< 3.0°/hr	< 3.0°/hr	At constant temperature using the Allan Variance method
Quiescent Noise	< 0.03°/s rms	< 0.03°/s rms	Over 3 - 30Hz
Bandwidth	> 30Hz	> 30Hz	55Hz typical to -3dB point
Cross Axis Sensitivity	< 2%	< 2%	–
Power Up Time	< 0.5s	< 0.5s	–
Current Dissipation	< 100mA	< 100mA	–
Inrush Current	< 200mA	< 200mA	–
Ref Output	2.4V ±0.02V	2.4V ±0.02V	w.r.t. GND over specified operating temperature range
Output Impedance	100 ±20ohms	100 ±20ohms	Rate and Ref. outputs
Minimum Output Current	> 500µA	> 500µA	Rate and Ref. outputs

4 Characteristics

Parameter	Minimum	Typical	Maximum	Notes	
Absolute Maximum Ratings					
Supply Voltage	0.00V	5.00V	5.50V	–	
Storage Temperature	-40°C	–	+85°C	See Note 1	
Operational Vibration	–	–	98m/s ²	20 to 2KHz peak to peak	
Shock Survival	–	–	–	See Note 2	
Operating Conditions					
Supply Voltage	4.75V	5.00V	5.25V	–	
Power Supply Noise	–	–	15.00mV rms	0.5 to 100Hz	
Temperature	CRS09A-01, CRS09A-11, CRS09A-02, CRS09A-12	-40°C	+23°C	+85°C	–
	CRS09A-22	-20°C	+23°C	+60°C	
Humidity	5%RH	–	95%RH	Not condensing	

5 Auxillary Output Signals

Parameter	Minimum	Typical	Maximum	Notes
Frequency				
Resonating Ring Frequency	27.4kHz	28.0kHz	28.6kHz	Output impedance 1kohm
Frequency Temperature Coefficient	-0.86Hz/°C	-0.80Hz/°C	-0.74Hz/°C	–
Temperature				
Temperature Sensor Scale Factor	-12.60mV/°C	-11.77mV/°C	-11.00mV/°C	Output impedance 470ohm

Note 1: The product must not be subjected to temperatures outside the recommended storage temperature range at any time.

Note 2: Do not drop the device onto a hard surface from a height exceeding 300mm.

6 Typical Performance Characteristics

Graphs showing typical performance characteristics for CRS09A are below.

Note: Typical data is with the device powered from a 5.0V supply, unless stated otherwise.

Bias Characteristics

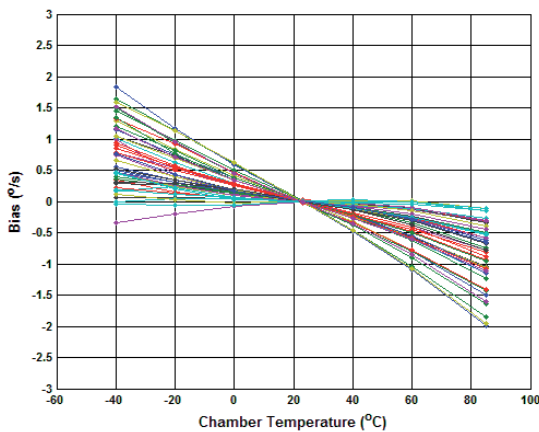


Figure 6.1 Bias Error over Temperature for CRS09A-01, including the Bias Setting Error at 23°C

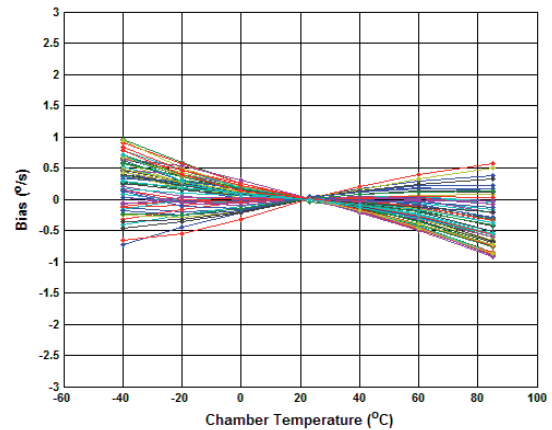


Figure 6.2 Bias Error over Temperature for CRS09A-11, including the Bias Setting Error at 23°C

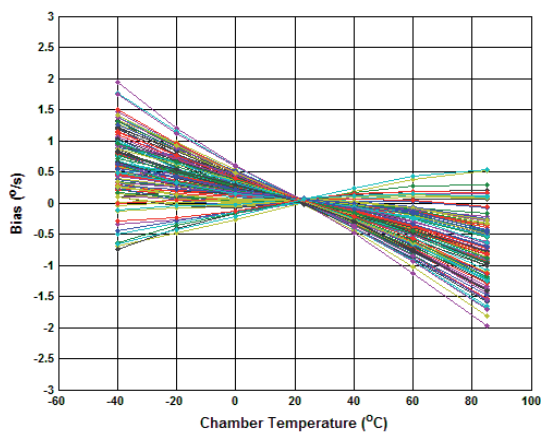


Figure 6.3 Bias Error over Temperature for CRS09A-02, including the Bias Setting Error at 23°C

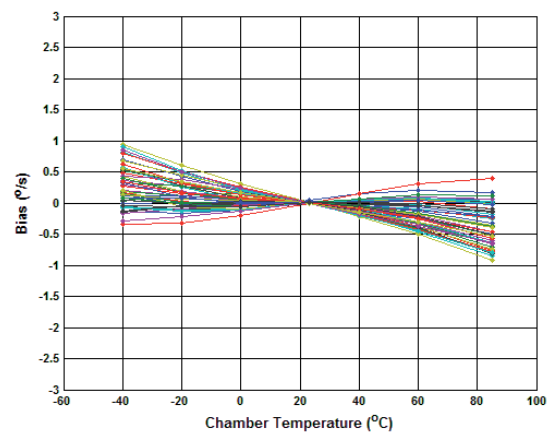


Figure 6.4 Bias Error over Temperature for CRS09A-12, including the Bias Setting Error at 23°C

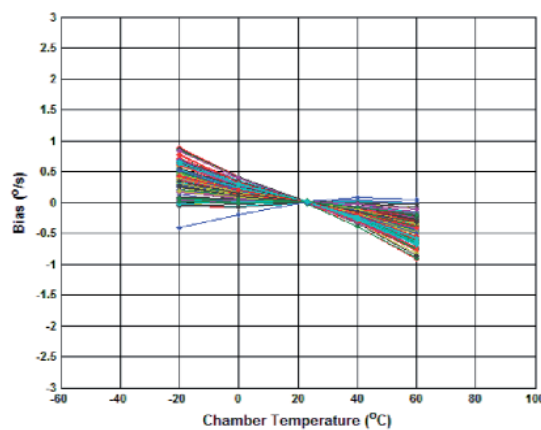


Figure 6.5 Bias Error over Temperature for CRS09A-22, including the Bias Setting Error at 23°C

Scale Factor Characteristics

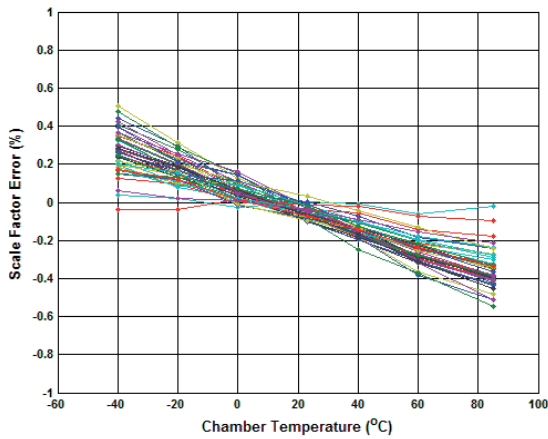


Figure 6.6 Scale Factor Error over Temperature for CRS09A-01, including the Setting Error at 23°C

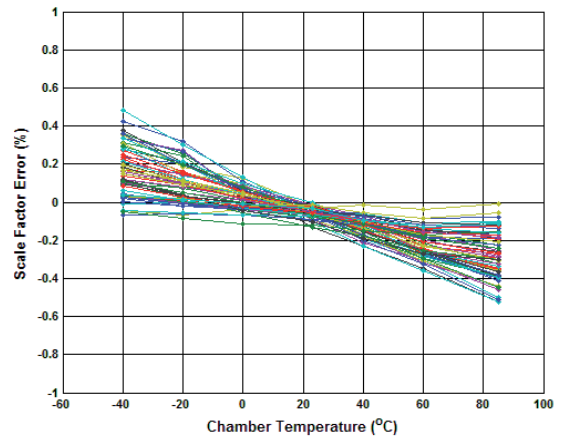


Figure 6.7 Scale Factor Error over Temperature for CRS09A-02, including the Setting Error at 23°C

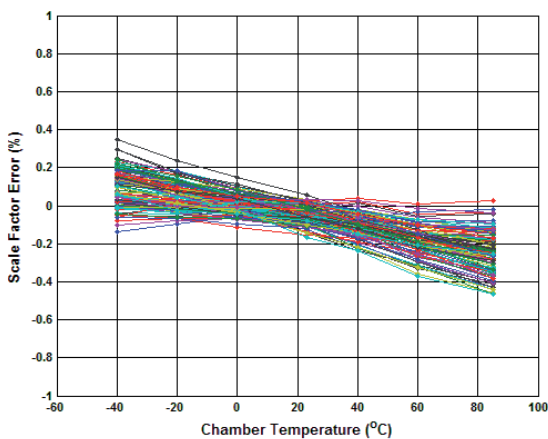


Figure 6.8 Scale Factor Error over Temperature for CRS09A-11, including the Setting Error at 23°C

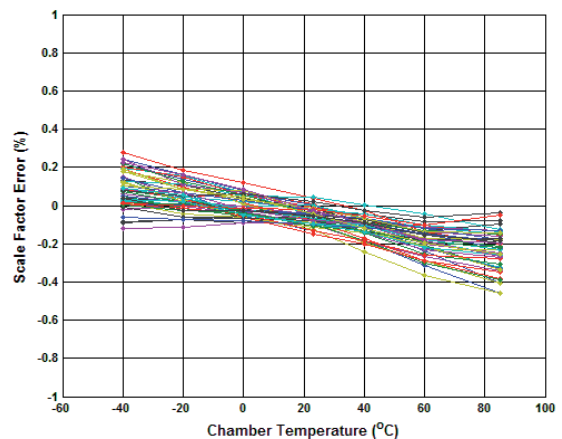


Figure 6.9 Scale Factor Error over Temperature for CRS09A-12, including the Setting Error at 23°C

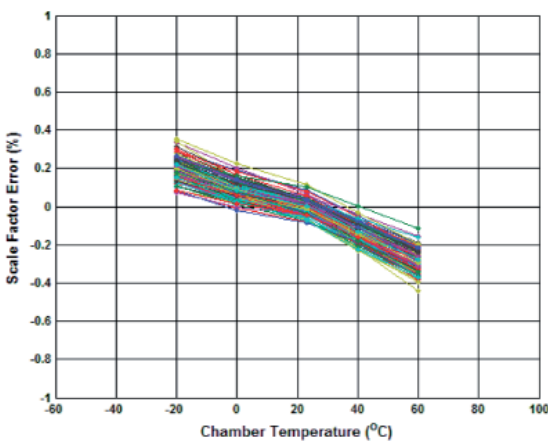


Figure 6.10 Scale Factor Error over Temperature for CRS09A-22, including the Setting Error at 23°C

Non-Linearity Error

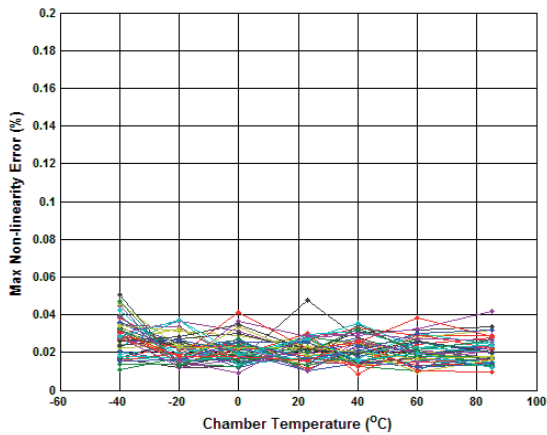


Figure 6.11 Non-Linearity Error (Maximum) over Temperature for CRS09A-01 and CRS09A-11

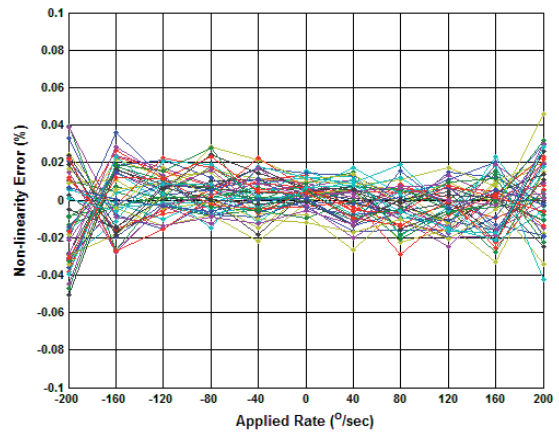


Figure 6.12 Non-Linearity Error versus Applied Rate at -40°C, CRS09A-01 and CRS09A-11

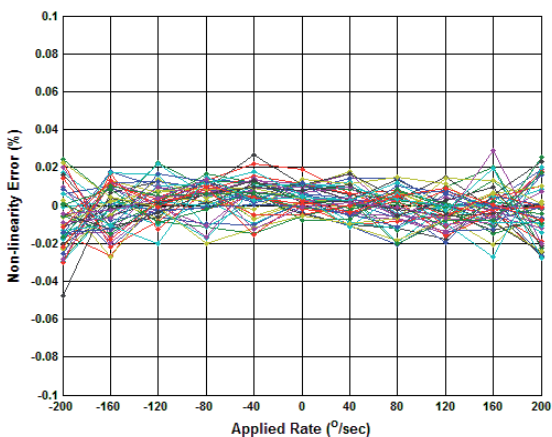


Figure 6.13 Non-Linearity Error versus Applied Rate at 23°C, CRS09A-01 and CRS09A-11

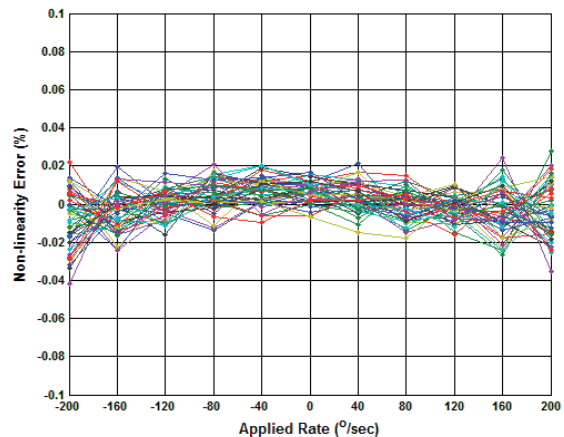


Figure 6.14 Non-Linearity Error versus Applied Rate at 85°C, CRS09A-01 and CRS09A-11

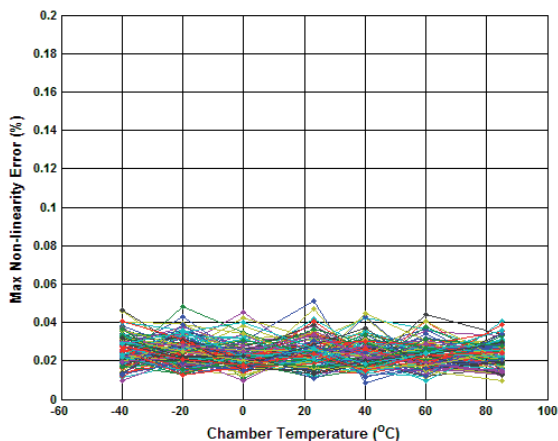


Figure 6.15 Non-Linearity Error (Maximum) over Temperature for CRS09A-02 and CRS09A-12

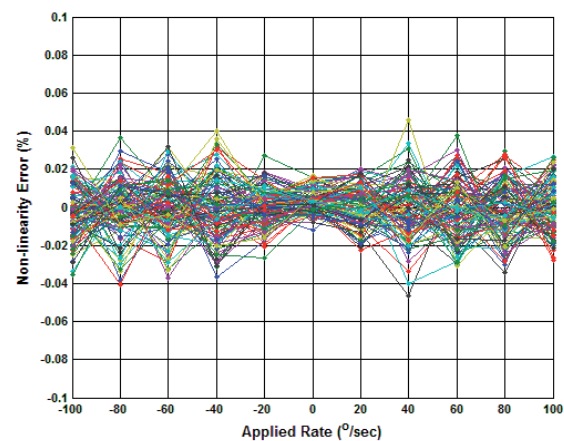


Figure 6.16 Non-Linearity Error versus Applied Rate at -40°C, CRS09A-02 and CRS09A-12

Non-Linearity Error Continued

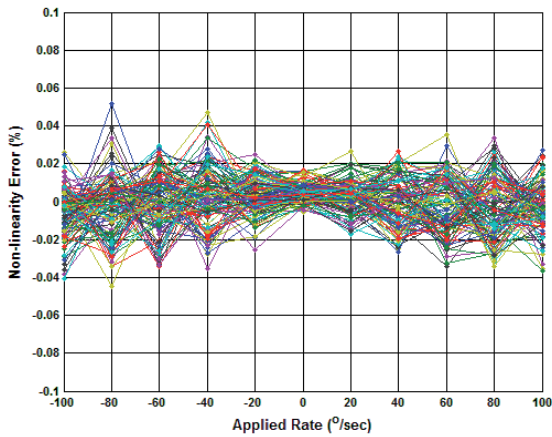


Figure 6.17 Non-Linearity Error versus Applied Rate at 23°C, CRS09A-02 and CRS09A-12

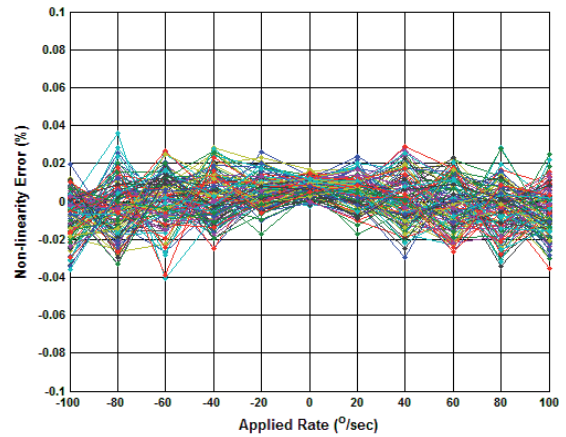


Figure 6.18 Non-Linearity Error versus Applied Rate at 85°C, CRS09A-02 and CRS09A-12

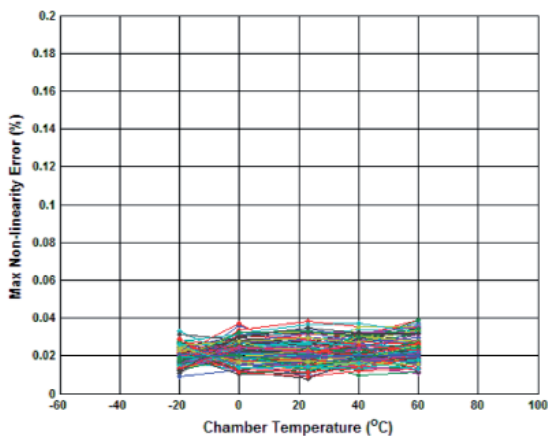


Figure 6.19 Non-Linearity Error (Maximum) over Temperature for CRS09A-22

Frequency Output

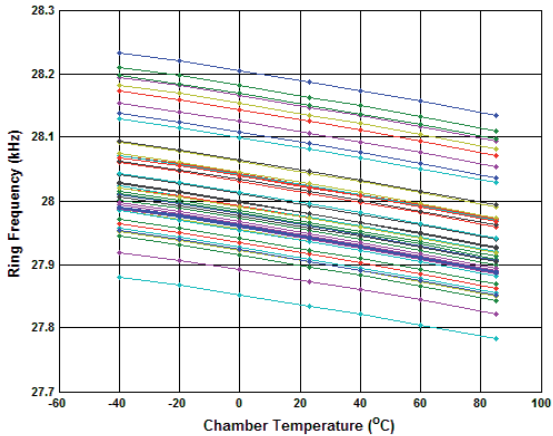


Figure 6.20 Frequency Output variation over Temperature for CRS09A-01

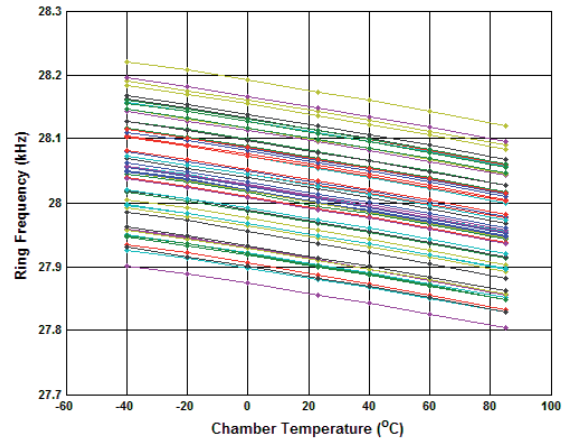


Figure 6.21 Frequency Output variation over Temperature for CRS09A-11

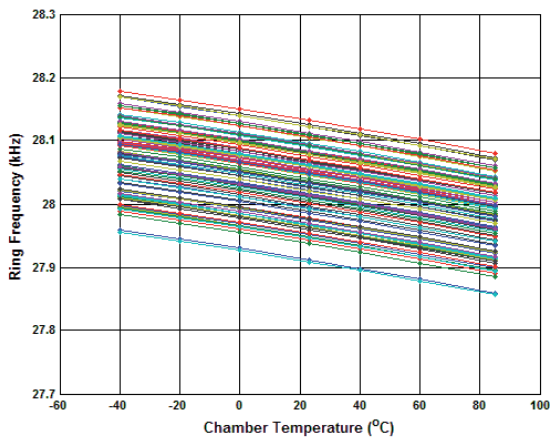


Figure 6.22 Frequency Output variation over Temperature for CRS09A-02

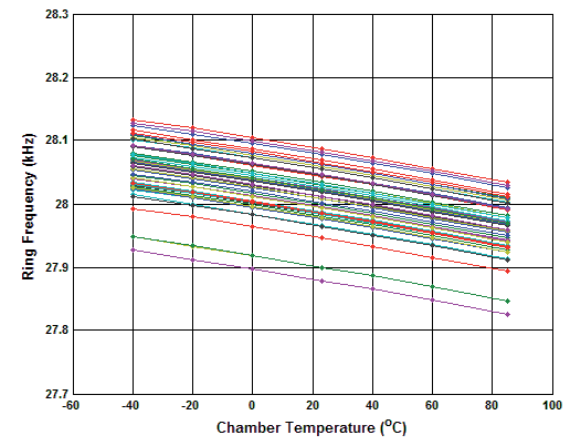


Figure 6.23 Frequency Output variation over Temperature for CRS09A-12

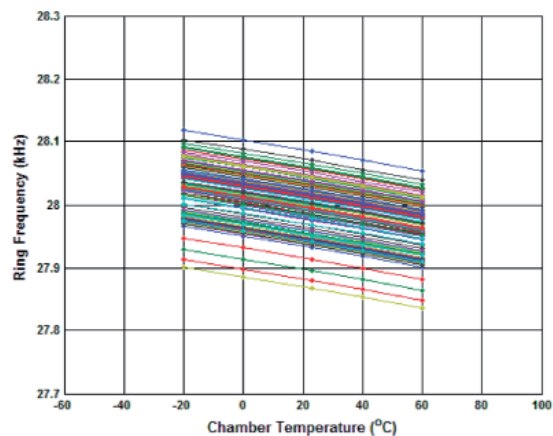


Figure 6.24 Frequency Output variation over Temperature for CRS09A-22

Allan Variance Data

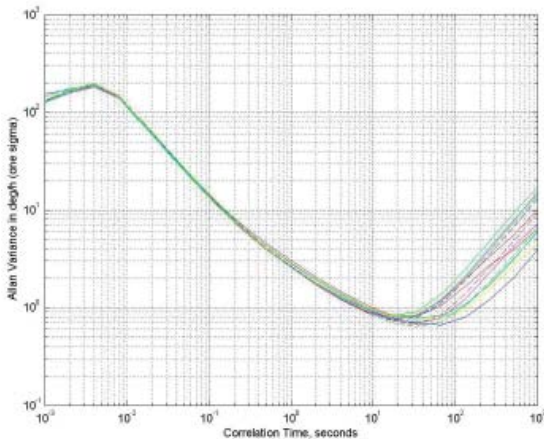


Figure 6.25 Typical Allan Variance Data for CRS09A-01 and CRS09A-11

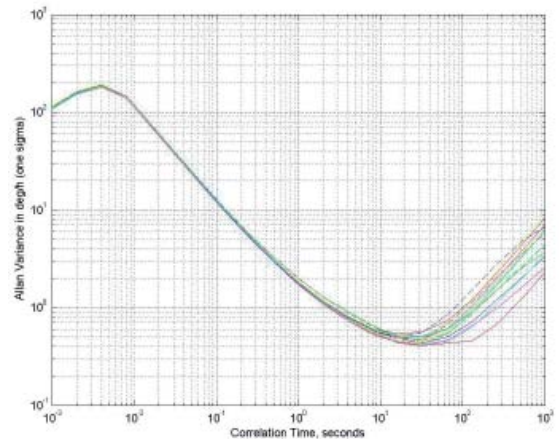


Figure 6.26 Typical Allan Variance Data for CRS09A-02 and CRS09A-12

Temperature Sensor Characteristics

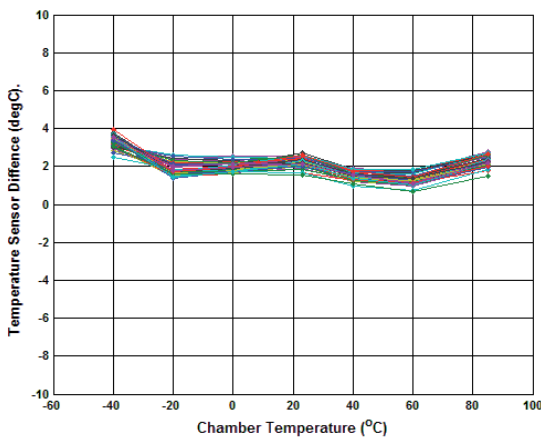


Figure 6.27 Temperature Sensor Error against Chamber Temperature for CRS09A-01 and CRS09A-11

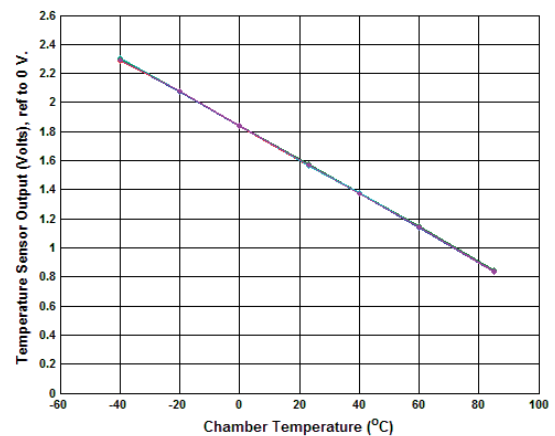


Figure 6.28 Temperature Sensor Output with respect to 0V (GND) against Chamber Temperature for CRS09A-01 and CRS09A-11

Temperature Sensor Characteristics Continued

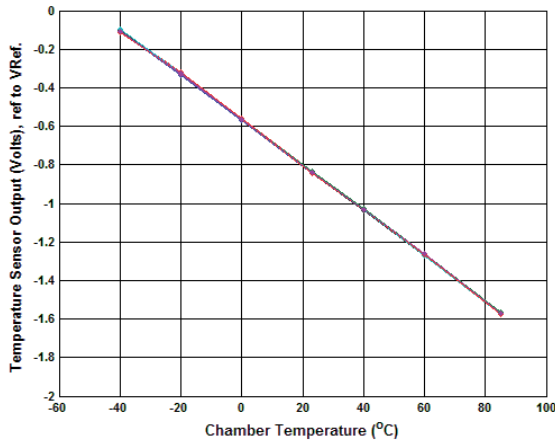


Figure 6.29 Temperature Sensor Output with respect to VRef against Chamber Temperature for CRS09A-01 and CRS09A-11

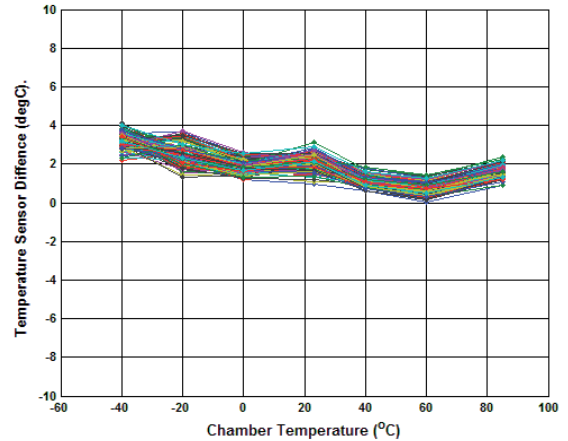


Figure 6.30 Temperature Sensor Error against Chamber Temperature for CRS09A-02 and CRS09A-12

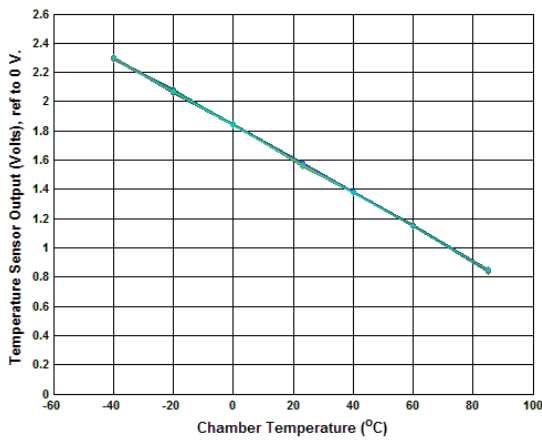


Figure 6.31 Temperature Sensor Output with respect to 0V (GND) against Chamber Temperature for CRS09A-02 and CRS09A-12

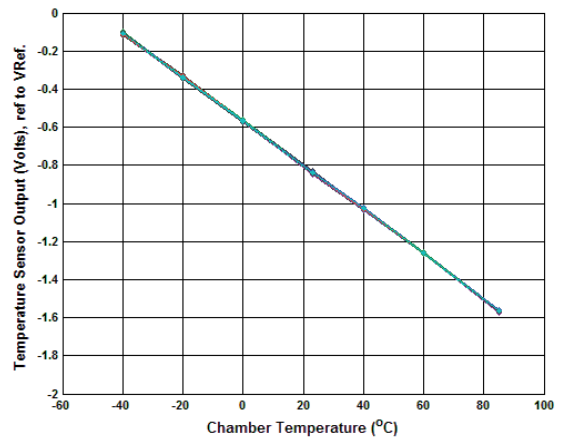


Figure 6.32 Temperature Sensor Output with respect to VRef against Chamber Temperature for CRS09A-02 and CRS09A-12

Voltage Reference Output (VRef)

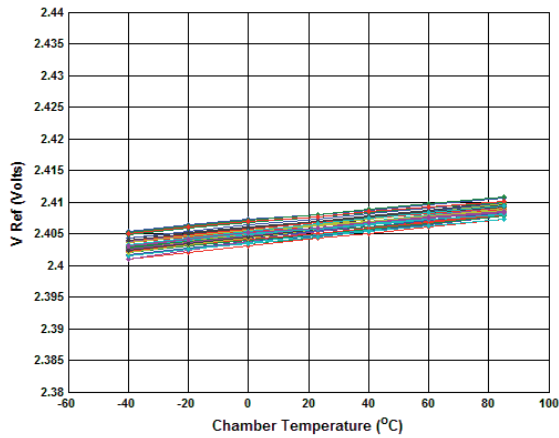


Figure 6.33 Voltage Reference variation with Temperature for CRS09A-01 and CRS09A-11

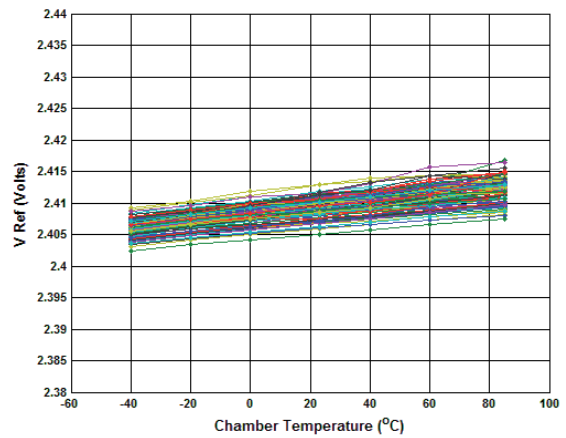


Figure 6.34 Voltage Reference variation with Temperature for CRS09A-02 and CRS09A-12

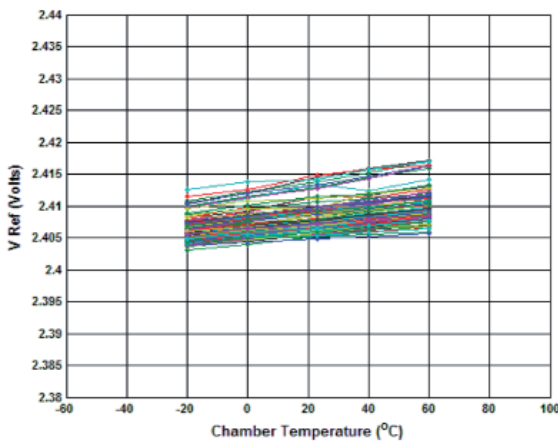


Figure 6.35 Voltage Reference variation with Temperature for CRS09A-22

Typical Current Consumption

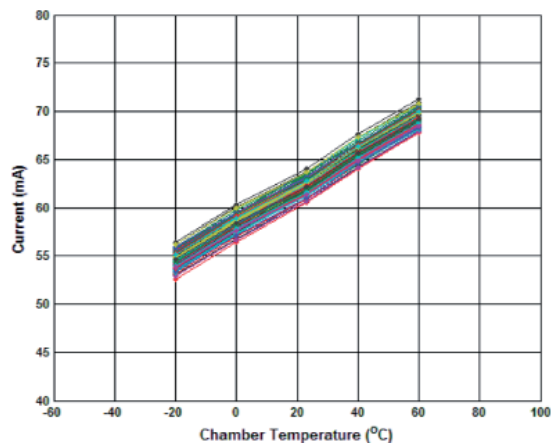


Figure 6.36 Current Consumption variation with Temperature for CRS09A-22

7 Interfacing

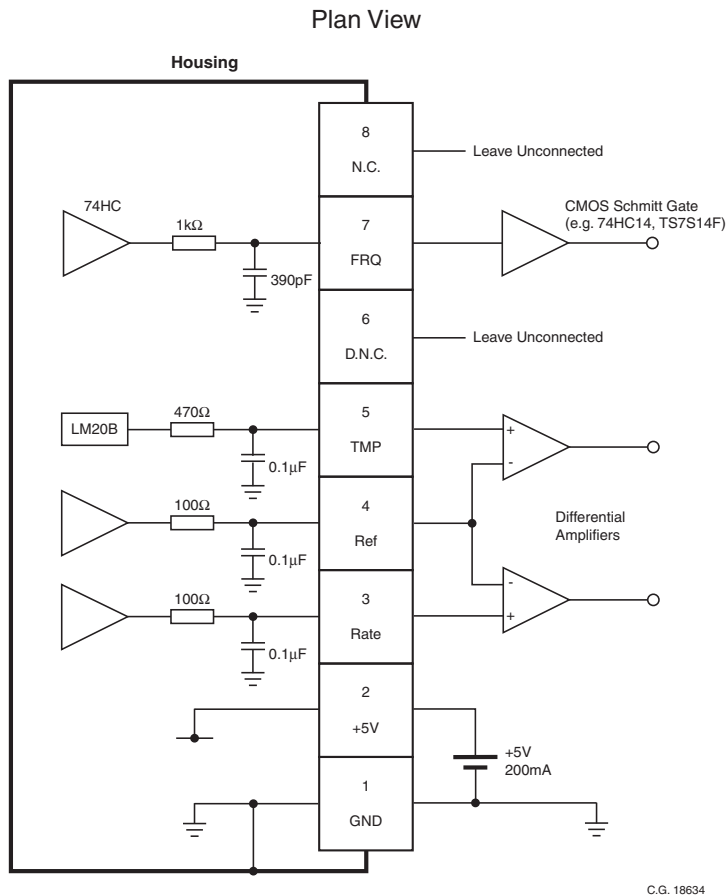


Figure 7.1a Recommended Interfacing

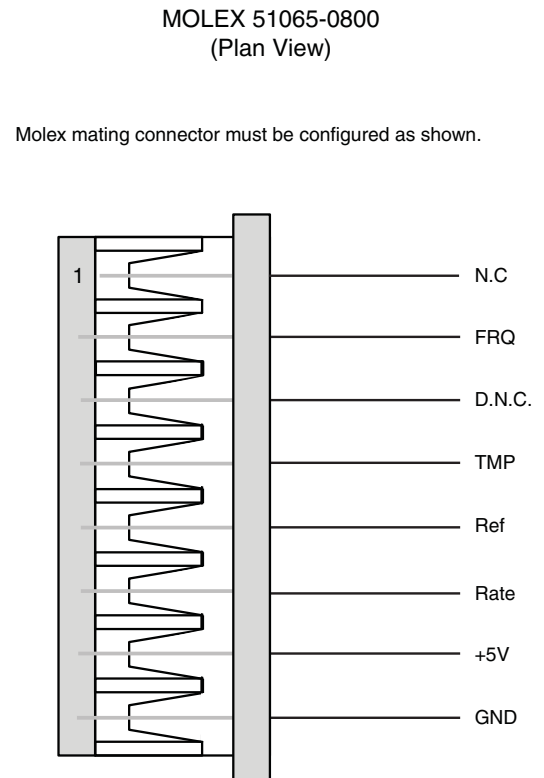


Figure 7.1b Molex Mating Connector Wiring Schedule

The table below provides connection details.

Connector Pin Number	Name	Comment
1	GND	Power Supply and Signal Ground, 0 Volts
2	Vcc	Power Rail: 4.75 to 5.25 Volts, at 100 mA approx. (200mA inrush)
3	Rate_Out	Angular Rate output. Nominally centred at 2.40 Volts for zero angular rate
4	Ref	Voltage reference. Nominally fixed at 2.40 Volts. This reference is derived from a precision voltage reference integrated circuit and is used as the reference for the analogue electronics
5	TMP	Temperature sensor output. A National Semiconductor LM20B is used to measure the temperature
6	D.N.C.	Do Not Connect to this pin
7	FREQ	This is CMOS Digital (74HC series) compatible digital output at two times the frequency of the sensor head
8	N.C.	No Connection: Do Not Connect to this pin

7.1 Temperature Sensor

The temperature sensor uses the LM20B device, internally connected as shown in Figure 7.2.

The output at 0°C is typically +1.864V with respect to GND. The temperature coefficient is typically -11.77 mV/°C.

The output can be measured with respect to GND or can be put through a differential input instrumentation amplifier, referenced to the Ref pin, in which case the offset at 0°C is typically -0.536V. At +25°C, the output is typically -0.830V with respect to Ref. The temperature sensors are not intended for use as a thermometer, since they are not calibrated on the Celsius scale. They are intended only as a temperature reference for thermal compensation techniques.

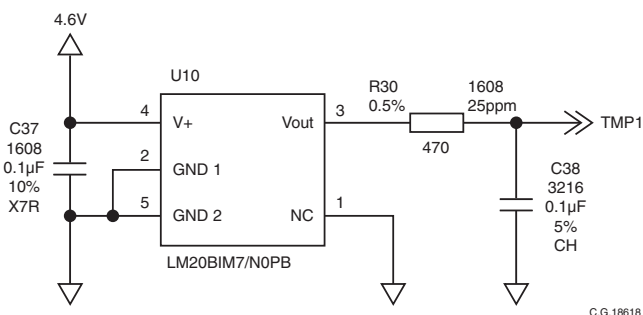


Figure 7.2 Temperature Sensors

7.2 Rate and Ref Outputs

Both the Rate and the Ref outputs are passed through a simple RC low pass filter before the output pins. The resistor value is 100 ohms. The capacitor value is 0.1 μ F.

It is recommended that the Rate Output (signal High or +) is differentially sensed using a precision instrumentation amplifier, referenced to the Ref output (signal Low or -).

The Offset of the instrumentation amplifier should be derived from the host stage (e.g. derived from the ADC Ref Voltage) or from the signal ground if the following stage is an analogue stage.

7.3 Frequency Outputs

This is CMOS Digital (74HC series) compatible digital output at two times the frequency of the sensor head. It is provided to give an indication of the temperature of the MEMS sensor head. The nominal frequency is 28 KHz with a typical temperature coefficient of -0.8 Hz/ $^{\circ}$ C.

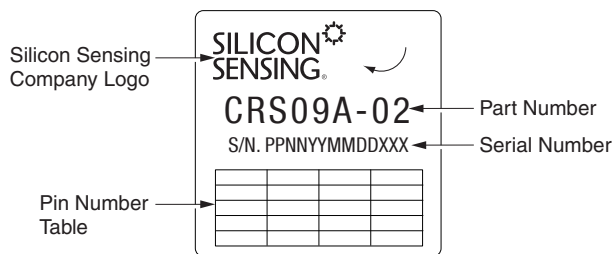
The signal is protected with a 1Kohm resistor before being output from the CRS09A. It is recommended that this signal is buffered with a CMOS Schmitt Gate such as 74HC12, or TC7S14F. The signal can be used to accurately measure the temperature of the MEMS structure.

An example of measuring the MEMS temperature is to use a precision crystal oscillator (operating at a very high frequency, for example 20, 40 or 60 MHz) to measure the frequency of the ring by measuring the time (oscillator clock cycles) to count to a defined number of ring cycles.

8 Glossary of Terms

ADC	Analogue to Digital Converter
ARW	Angular Random Walk
BW	Bandwidth
C	Celsius or Centigrade
DAC	Digital to Analogue Converter
DPH	Degrees Per Hour
DPS	Degrees Per Second
DRIE	Deep Reactive Ion Etch
EMC	Electro-Magnetic Compatibility
ESD	Electro-Static Damage
F	Farads
h	Hour
HBM	Human Body Model
Hz	Hertz, Cycle Per Second
K	Kilo
MEMS	Micro-Electro Mechanical Systems
mV	Mili-Volts
NEC	Not Electrically Connected
NL	Scale Factor Non-Linearity
PD	Primary Drive
PP	Primary Pick-Off
RC	Resistor and Capacitor filter
s	Seconds
SF	Scale Factor
SMT	Surface Mount Technology
SOG	Silicon On Glass
SD	Secondary Drive
SP	Secondary Pick-Off
T.B.A.	To Be Announced
T.B.D.	To Be Described
V	Volts

9 Part Markings



C.G. 18814

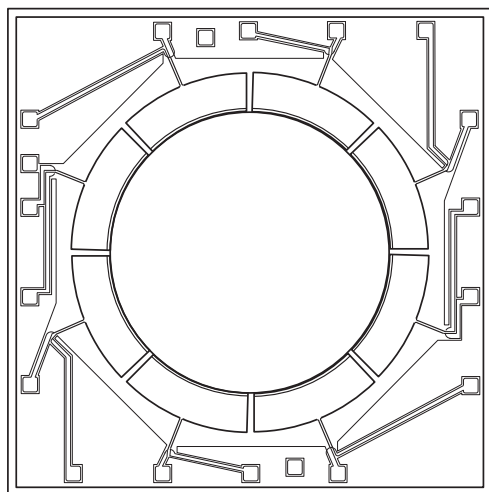
Figure 9.1 Part Marking

	Code	Range
Product Type	PP	9A
Device Type	NN	01, 02, 11, 12 or 22
Year Number	YY	00 - 99
Month Number	MM	01 - 12
Day Number	DD	01 - 31
Serial Number	XXX	001 - 999

Table 9.1 Serial Number Code

10 Silicon MEMS Ring Sensor (Gyro)

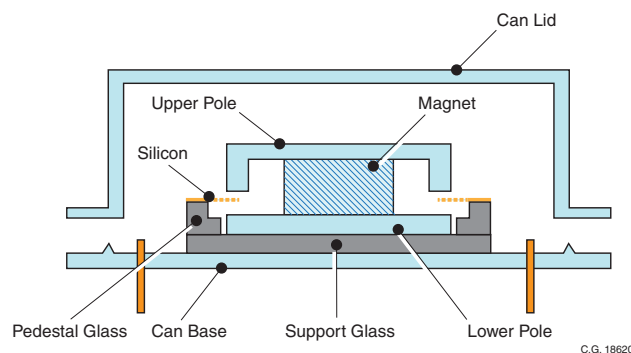
The silicon MEMS ring is 6mm diameter by 100µm thick, fabricated by Silicon Sensing Systems using a DRIE (Deep Reactive Ion Etch) bulk silicon process. The ring is supported in free-space by sixteen pairs of 'dog-leg' shaped symmetrical legs which support the ring from the supporting structure on the outside of the ring.



C.G. 18619

Figure 10.1 Silicon MEMS Ring

The bulk silicon etch process and unique patented ring design enable close tolerance geometrical properties for precise balance and thermal stability and, unlike other MEMS gyros, there are no small gaps to create problems of interference and stiction. These features contribute significantly to CRS09A's bias and scale factor stability over temperature, and vibration immunity. Another advantage of the design is its inherent immunity to acceleration induced rate error, or 'g-sensitivity'.



C.G. 18620

Figure 10.2 MEMS Sensor Head

The ring is essentially divided into 8 sections with two conductive tracks in each section. These tracks enter and exit the ring on the supporting legs. The silicon ring is bonded to a glass pedestal which in turn is bonded to a glass support base. A magnet, with upper and lower poles, is used to create a strong and uniform magnetic field across the silicon ring. The complete assembly is mounted within a hermetic can with a high internal vacuum.

The tracks along the top of the ring form two pairs of drive tracks and two pairs of pick-off tracks. Each section has two loops to improve drive and pick-off quality.

One pair of diametrically opposed tracking sections, known as the Primary Drive PD section, is used to excite the $\cos 2\theta$ mode of vibration on the ring. This is achieved by passing current through the tracking, and because the tracks are within a magnetic field causes motion on the ring. Another pair of diametrically opposed tracking sections is known as the Primary Pick-off PP section is used to measure the amplitude and phase of the vibration on the ring. The Primary Pick-off sections are in the sections 90° to those of the Primary Drive sections. The drive amplitude and frequency is controlled by a precision closed loop electronic architecture with the frequency controlled

by a Phase Locked Loop (PLL), operating with a Voltage Controlled Oscillator (VCO), and amplitude controlled with an Automatic Gain Control (AGC) system. The primary loop therefore establishes the vibration on the ring and the closed loop electronics is used to track frequency changes and maintain the optimal amplitude of vibration over temperature and life. The loop is designed to operate at about 14kHz.

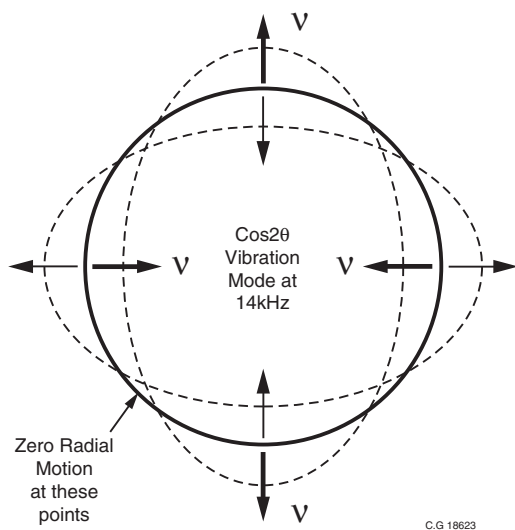


Figure 10.3 Primary Vibration Mode

Having established the $\cos 2\theta$ mode of vibration on the ring, the ring becomes a Coriolis Vibrating Structure Gyroscope. When the gyroscope is rotated about its sense axis the Coriolis force acts tangentially on the ring, causing motions at 45° displaced from the primary mode of vibration. The amount of motion at this point is directly proportional to the rate of turn applied to the gyroscope. One pair of diametrically opposed tracking sections, known as the Secondary Pick-off SP section, is used to sense the level of this vibration. This is used in a secondary rate nulling loop to apply a signal to another pair of secondary sections, known as the Secondary Drive SD. The current applied to the Secondary Drive to null the secondary mode of vibration is a very accurate measure of the applied angular rate. All of these signals occur at the resonant frequency of the ring. The Secondary Drive signal is demodulated to baseband to give a voltage output directly proportional to the applied rate in free space.

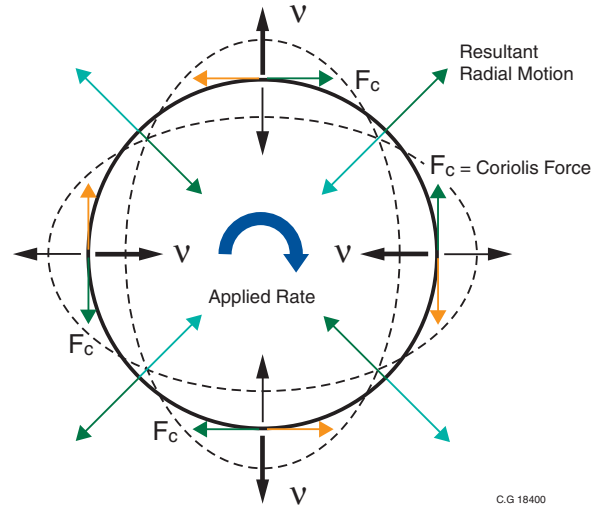


Figure 10.4 Secondary Vibration Mode

The closed loop architecture on both the primary and secondary loops result in excellent bias, scale factor and non-linearity control over a wide range of operating environments and life. The dual loop design, introduced into this new Sensor Head design, coupled with improved geometric symmetry results in excellent performance over temperature and life. The discrete electronics employed in CRS09AA, ensures that performance is not compromised.

CRS09A Technical Datasheet

Analogue Angular Rate Sensor

High Performance MEMS Gyroscope



www.siliconsensing.com

Notes

Silicon Sensing Systems Limited
Clifford Road Southway
Plymouth Devon
PL6 6DE United Kingdom

T: +44 (0)1752 723330
F: +44 (0)1752 723331
E: sales@siliconsensing.com
W: siliconsensing.com

Silicon Sensing Systems Japan Limited
1-10 Fuso-Cho
Amagasaki
Hyogo 6600891 Japan

T: +81 (0)6 6489 5868
F: +81 (0)6 6489 5919
E: sssj@spp.co.jp
W: siliconsensing.com

Specification subject to change without notice.

© Copyright 2017
Silicon Sensing Systems Limited
All rights reserved.

Printed in England 09/2017
Date 19/09/2017

CRS09A-00-0100-132 Rev 4
DCR No. 710013559